**"A Cochlear Nucleus Auditory
prosthesis based on microstimulation"**

Contract No. **No. NO1-DC-4-0005**
Progress Report #8

HUNTINGTON MEDICAL RESEARCH INSTITUTES
NEURAL ENGINEERING LABORATORY
734 Fairmount Avenue
Pasadena, California 91105

D.B. McCreery, PhD

HOUSE EAR INSTITUTE
2100 WEST THIRD STREET
Los Angeles, California 90057

R.V. Shannon PhD
S. Otto M.S.
M. Waring, PhD

SUMMARY

Studies were initiated in 2 cats with silicon substrate microstimulating arrays chronically implanted in their cochlear nuclei. The objective was to determine if stimulation-induced depression of neuronal excitability (SIDNE), which always accompanies high-rate stimulation, is more severe when multiple, closely-spaced microelectrodes are pulsed. The severity of SIDNE was assessed as changes in the response growth functions of the compound neuronal responses evoked by the microelectrodes in the cochlear nucleus and recorded in the contralateral inferior colliculus. In both animals, the severity of the SIDNE was the same after 2 days of prolonged pulsing when either 1, 2, 8 or 13 electrode sites were pulsed. Microelectrode sites that were not subjected to prolonged pulsing, but adjacent to those that were pulsed, exhibited no SIDNE. In the feline cerebral cortex, SIDNE can be minimized by employing a stimulus regimen in which the inherent spatial resolution of the array is maximized (sequential pulsing at an amplitude in which there is minimal overlap of the effective current fields), and it is possible that we were approximating these conditions in the cochlear nucleus.

In the past quarter, three patients with penetrating brainstem implants underwent their follow-up testing. Two patients implanted with second-generation penetrating microelectrode arrays, in which 2 of the electrodes are longer than in the first generation devices, experience marked nonauditory side effects in the form of sharp facial pain when the long electrodes were pulsed, suggesting that the long microelectrodes were stimulating axons into the descending trigeminal tract. One of the patients (PABI#6) derives significant suggestive benefit from his penetrating microelectrodes and has resumed regular use of the device, after the offending electrodes were removed from his map. Patient #7 also reported the same facial pain when the long electrodes were pulsed and also reported some unusual vertigo associated with 2 of the electrodes in his surface array. He has been advised to discontinue use of his implant pending full integrity testing of the device.

1: Work completed at HMRI
 Evaluation of a multi-site silicon-substrate microstimulating array
INTRODUCTION

The work scope of our contract calls for the development of arrays of silicon substrate electrodes, which should allow placement of many more electrode sites within the human cochlear nucleus than is possible with discrete iridium microelectrodes. Recently we have demonstrated that an array of silicon-substrate electrodes can introduce at least 16 channels of acoustic information into the feline ventral cochlear nucleus (McCreery et al, 2006, QPR #7). However, prolonged high-rate microstimulation in the feline cochlear nucleus can induce a prolonged but reversible depression of neuronal excitability (McCreery et al, 2000). In the cerebral cortex, this "SIDNE" is greater and more prolonged when many closely-spaced microelectrodes are pulsed, either simultaneously or sequentially (McCreery et al, 2002). That study also showed that the SIDNE can be minimized by employing a stimulus regimen in which the inherent spatial resolution of the array is maximized (sequential pulsing at an amplitude in which there is minimal overlap of the effective current fields).

During the last quarter, we have begun to evaluate the stimulating-induced depression of neuronal excitability during prolonged microstimulation at multiple sites in the feline ventral cochlear nucleus.
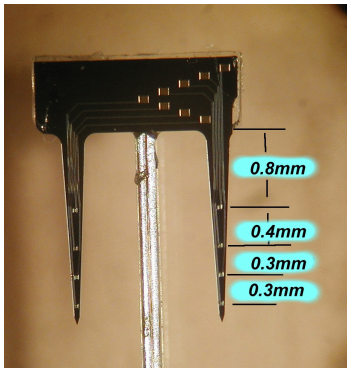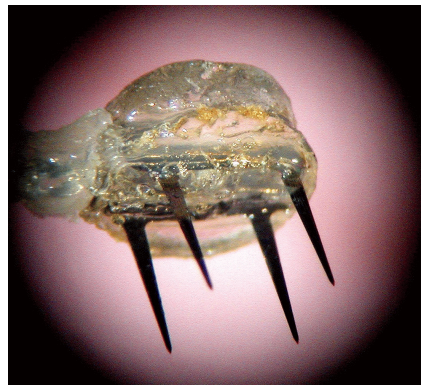

Figure 1A

Figure 1B

METHODS

Figure 1A shows a multisite silicon substrate probe with 2 shanks and 8 stimulating sites sputter-coated with iridium oxide. The probes were fabricated at the University of Michigan under the direction of Design Engineer Jamile Hetke. The 4 electrode sites on each shank are located 0.8 to 1.7 mm below the probe's transverse spine. After bonding of the Parylene-coated gold lead wires the transverse spines of two probes were encapsulated in EpoTek 301 epoxy to form the button superstructure, 2.5 mm in diameter. A complete array of 2 probes (4 shanks and 16 electrode sites) extending from the epoxy superstructure is shown in figure 1B.

Studies were conducted in two cats, CN157 and CN158, in which the silicon-substrate array had been implanted in the cochlear nucleus for 180 and 35 days, respectively. In phase 1, one microelectrode site (CN157) or two widely-separated microelectrode sites (CN158) were pulsed continuously for 8 hours on two successive days, using the stimulus regimen described below. Beginning approximately 60 hours after the end of phase 1, 8 sites (CN157) or 13 sites (CN158) were pulsed sequentially (interleaved stimulation) for 8 hours on two successive days. Immediately before, and immediately after phases 1 and 2, response growth functions of the compound neuronal activity evoked from each sites in the VCN were recorded via the electrode implanted in the contralateral inferior colliculus. The changes in the thresholds and slopes RGFs between the beginning and end of each phase are indices of the severity of the SIDNE produced by the two stimulation regimens.

For the prolonged stimulation regimen, we have simulated an acoustic environment based on a computer-generated artificial voice that was specified and provided by the

International Telegraphic & Telephony Consultive Convention, for the purpose of testing telecommunication equipment (CCITT, 1988). The CCITT artificial voice reproduces many of the characteristics of real speech, including the long-term average spectrum, the short-term spectrum, the instantaneous amplitude distribution, the voiced and unvoiced structure of speech, and the syllabic envelope. The artificial voice signal was passed through a full wave rectifier and then underwent logarithmic amplitude compression, before being sent through an appropriate anti-aliasing filter (McCreery et al, 2000). The amplitude of the signal from the filter then sets the amplitude of the charge-balanced stimulus pulses, which were delivered sequentially to each electrode at 250 Hz (per electrode), in 256 steps of amplitude. One step above acoustic silence was represented by a stimulus of 10 µA, which was the threshold of the RGFs evoked from channel 16 of cat CN158 and channel 13 of cat CN157 (the channels with the highest thresholds).   Thus the stimulus ranged in amplitude from 10 to 30 µA (1.5 to 4.5 nC/phase with a pulse duration of 150 µs/phase). The artificial voice signal was presented for 15 seconds, followed by 15 seconds in which the stimulus amplitude was held at 10 µA. This 50% duty cycle is intended to simulate a moderately noisy acoustic environment. Each of the pulsed electrodes received the same stimulus, but the stimulus was interleaved across the array. Similar parameters produce moderate SIDNE in the feline cochlear nucleus during prolong pulsing with a single discrete iridium microelectrode (McCreery et al, 1997, 2000). The stimulation and data acquisition were conducted using a two-way radiotelemetry stimulation and data acquisition system, and the cats are able to move about freely in a large Lucite cage. This telemetry system and its companion software allow continuous monitoring of the voltage waveform across the stimulating microelectrodes, and of the compound evoked potential induced in the inferior colliculus by the stimulating microelectrodes.

Recording of compound evoked responses

The responses evoked from each of the microelectrode sites in the CN were recorded via the electrode in the rostral pole of the contralateral inferior colliculus. The cat was lightly anesthetized with Propofol and the recordings were conduced inside a double-wall sound isolation booth (Audiometrics 120A-SP). The stimulus was cathodic-first, charge-balanced pulse pairs, each phase 150 µs in duration, ranging from 0 to 30 µA. 512 to 2048 successive responses were averaged to obtain each averaged evoked compound action potential (AECAP). The response growth functions, which represent the recruitment of the neurons surrounding each stimulating microelectrode in the VCN, were generated by plotting the amplitude of the first component of each of the AECAPs against the amplitude of the stimulus. The latency to the onset of the first component of the AECAP is approximately 1 ms, and thus we assume that it represents the activity of neurons excited by the microstimulation in the CN and projecting directly to the contralateral inferior colliculus.

RESULTS

Figure 2 shows the relative positions of the microstimulating sites in cats CN157 and CN158 that were pulsed in phases 1 and 2 . Both cats remain alive, and thus the anatomical locations of the probe shanks in the cochlear nucleus have not been confirmed, but all shanks probably are in the posteroventral cochlear nucleus. In cat CN158, 12 of the microstimulating sites produced large evoked responses in the contralateral inferior colliculus (electrical continuity to sites 1,7 & 10 was intermittent, probably due to damage to the percutaneous connector, and these sites were not used)**.** The RGFs of the early component of the AECAP recorded in the IC are shown in figure 3. In phase 1, when only sites 4 and 15 were pulsed, the RGFs from the unpulsed sites were very stable, as were the RGFs from pulsed site 4 (The

RGFs from before and after phase 1 are nearly identical). The threshold of the RGF from pulsed site 15 did increase to approximately 10 µA. This effect of the artificial voice signal has been observed previously, in which the threshold of the response tends to increase to approximately the lower end of the range of the artificial voice signal (in this case, 10 µA). In phase 2, in which 13 sites were pulsed, this behavior was evident for all 9 sites whose RGFs were recorded. Thus the sites whose evoked response initially exhibited the highest thresholds exhibited the largest SIDNE (e.g., the sites on the rostral- lateral shank, which probably is in the rostral-lateral posteroventral cochlear nucleus). By the end of phase 2, the RGFs from all sites still spanned the full range of the artificial voice signal (10 to 30 µA). However, the slope of the RGF from site 15 was slightly less after phase 2 than after phase 1, suggesting some synergistic effect due to stimulating with many closely-spaced sites.

The results were similar for cat CN157 (Figure 4) , in which microstimulating site 9 was pulsed in phase 1 and 8 adjacent sites were pulsed in phase 2. In both animals, the evoked responses recorded at the end of phases 1 and 2 spanned the full range of the artificial voice signal, whether 1, 2, 8 or 13 sites were subjected to prolong pulsing. In the cat sensorimotor cerebral cortex, the SIDNE may be much greater when many closely-spaced microelectrodes are pulsed (McCreery et al, 2002). In the cochlear nucleus, we observed only a hint of this phenomenon, in the small decrease in the slope of the RGF from site 15 in cat CN158. In the cerebral cortex, the SIDNE can be minimized by employing a stimulus regimen in which the inherent spatial resolution of the array is maximized (sequential pulsing at an amplitude in which there is minimal overlap of the effective current fields), and it is possible that we were approximating this condition in the cochlear nucleus, in which the charge per phase did not exceed 4.5 nC/phase. In the present generation of penetrating microelectrodes for clinical use, the electrode surface area has been increased in order to allow a maximum of 8 nC/phase, and one patient (PABI #6) is using the full range. In the next quarter, we will repeat the studies described above in cats CN157 and CN158, using the artificial voice with a wider range of stimulus amplitude, and also by increasing the duty cycle of the artificial voice signal, to modeling a noisier acoustic environment.

REFERENCES
1.   **McCreery DB, Yuen TG, Agnew WF, and Bullara LA.** A characterization of the effects on neuronal excitability due to prolonged microstimulation with chronically implanted microelectrodes. *IEEE Trans Biomed Eng* 44: 931-939, 1997.
2.   **McCreery DB, Yuen TG, and Bullara LA.** Chronic microstimulation in the feline ventral cochlear nucleus: physiologic and histologic effects. *Hear Res* 149: 223-238, 2000.
3.   **McCreery DB, Agnew WF, and Bullara LA.** The effects of prolonged intracortical microstimulation on the excitability of pyramidal tract neurons in the cat. *Ann Biomed Eng* 30: 107-119., 2002.
4.   **McCreery D, Lossinsky A, and Pikov V.** Performance of multisite silicon microprobes implanted chronically in the ventral cochlear nucleus of the cat. *Submitted to IEEE Trans Biomed Engr*, 2006.
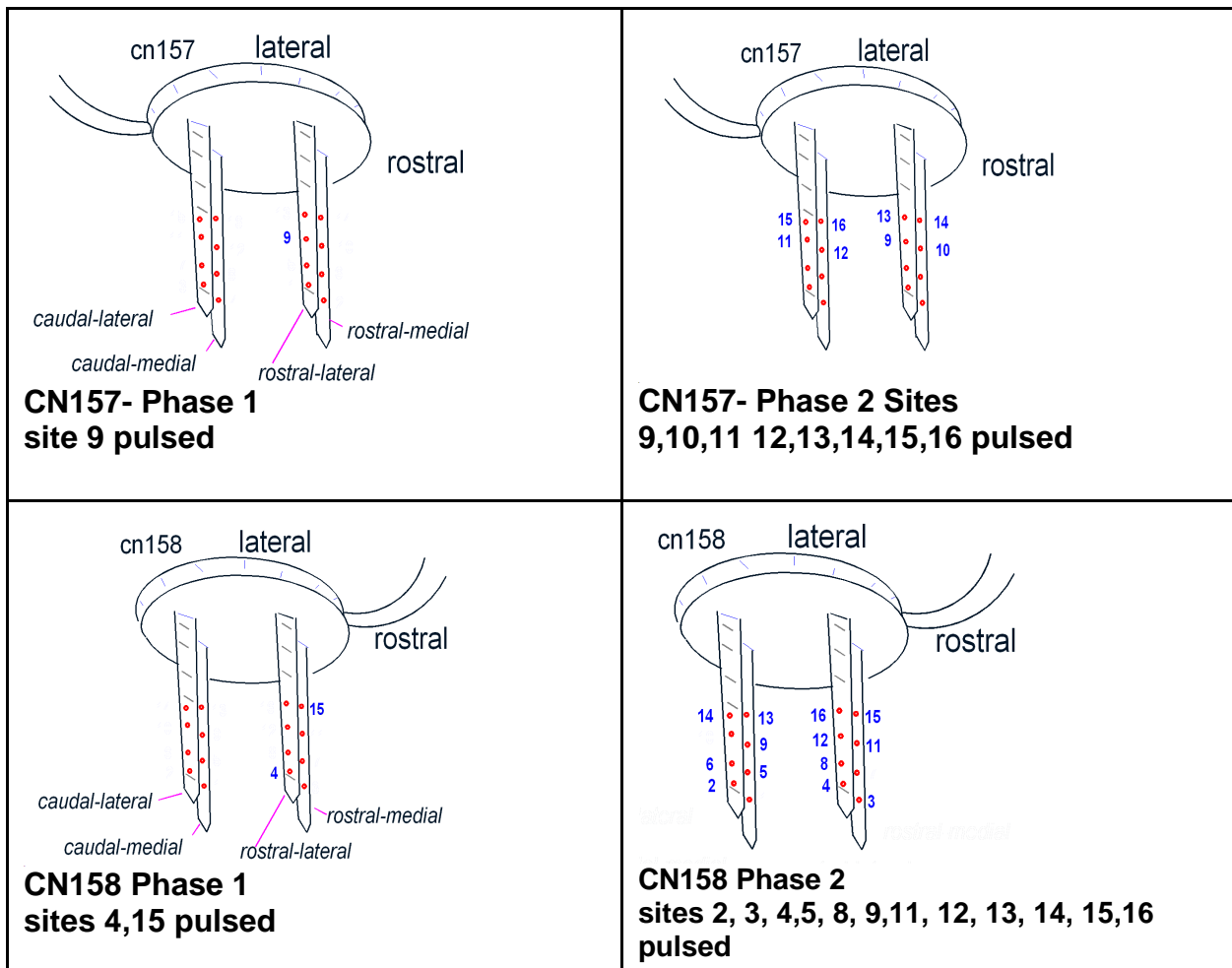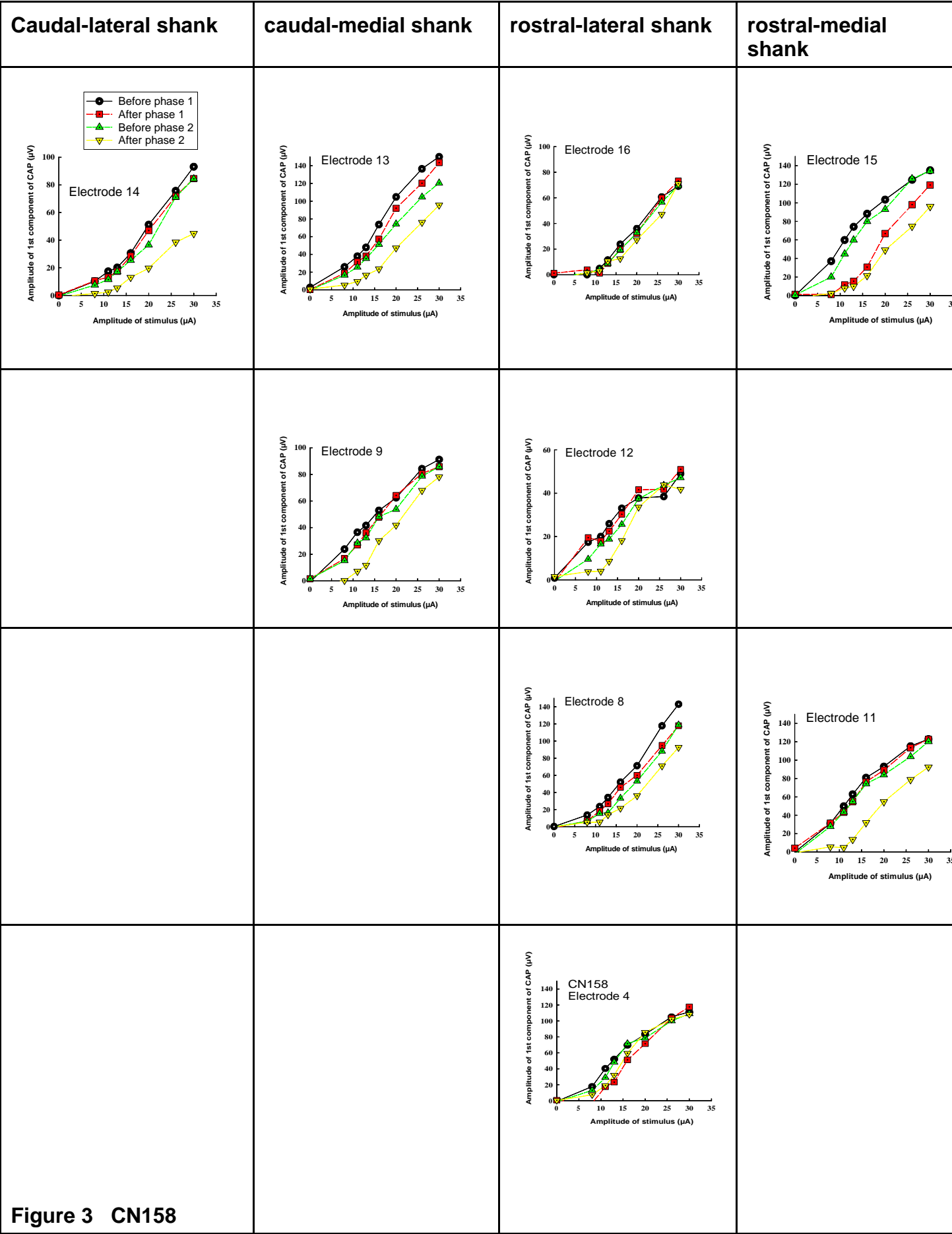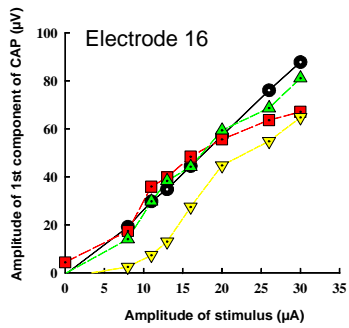
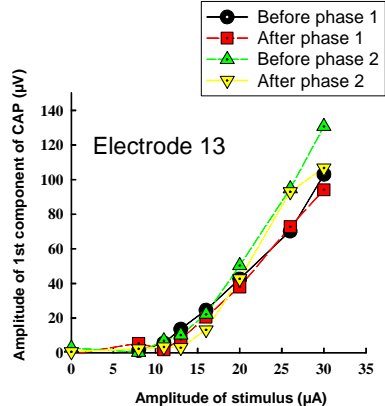**CN157- Phase 1
site 9 pulsed**

**CN157- Phase 2 Sites
9,10,11 12,13,14,15,16 pulsed**

**CN158 Phase 1
sites 4,15 pulsed**

**CN158 Phase 2
sites 2, 3, 4,5, 8, 9,11, 12, 13, 14, 15,16
pulsed**

Figure 2

Caudal-lateral shank	caudal-medial shank	rostral-lateral shank	rostral-medial shank
Figure 3 CN158			
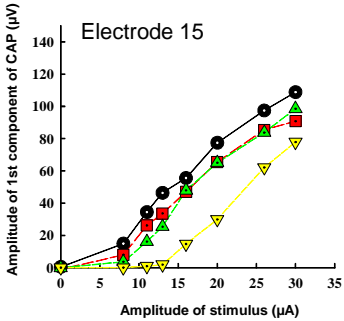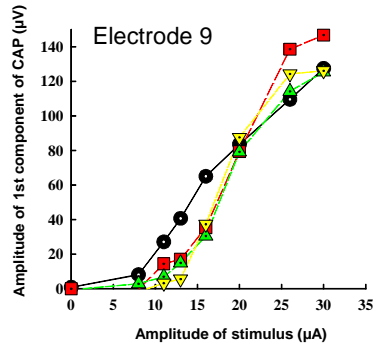
Figure 3   CN158

Caudal-lateral shank	caudal-medial shank	rostral-lateral shank	rostral-medial shank
	Electrode 16	Electrode 13	
Electrode 15 **Figure 4 CN157**		Electrode 9	

II. **Evaluations of patients with penetrating auditory brainstem implants**
**Overview**

   To date, auditory brainstem implants (ABIs) that include the array of penetrating microstimulating electrodes (PABI) have been implanted into 8 patients afflicted with type 2 neurofibromatosis (NF2), after removal of the acoustic tumors. PABI patients 6, 7, & 8 have received the 2nd generation devices, with 10 penetrating microelectrodes, including 2 microelectrodes with tip sites 2.5 mm below the epoxy superstructure (deeper than in the first generation device). In the 2nd generation device, the surface areas of all penetrating electrodes have been increased to 5000 sq. microns, to allow a maximum charge per phase of 8 nC.

FIG 1: PABI #6 Threshold and MCL

$\triangle$ Surface L 300 uS/ph
$\bigcirc$ Surface R 300 uS/ph
$\blacktriangle$ Penetrating 25 uS/ph

         In this quarter we saw PABI#6 for his 3-month follow-up visit, PABI#7 for initial stimulation visit, and were scheduled to see PABI#8 for her initial stimulation. However, an unanticipated adverse event changed the schedule for these three PABI patients, as detailed below. None of the previous PABI patients were seen in this quarter.

PABI#6

   PABI #6 returned for his 3-month follow-up visit on 26 April 2006. His thresholds and maximum comfort levels were generally stable (Figure 1). In this diagram, the threshold for an auditory percept and maximum comfort level from a particular testing session are connected by a vertical line, and data for each electrode from the first and 2nd testing sessions are shown slightly displaced along the abscissa. He reported an unpleasant non-auditory side

Fig 2: PABI Speech Recognition over Time

effect (NASE) on electrode 20, one of the long electrodes, which increased in severity during the first three months that he used his speech processor at home. It increased to the point where he could not use that program. The NASE was a sharp pain localized to the ipsilateral face. In the lab we repeated the threshold measure on electrode 20 and he received the same strong and unpleasant NASE even at the lowest stimulation level, approximately 0.25 nC. Jean Moore, our anatomical consultant, suggested that the NASE symptoms were consistent with activation of the spinal nucleus of the trigeminal nerve, producing a sensation similar to that described by patients with trigeminal neuralgia. This presents somewhat of a paradox, since the descending trigeminal tract should be approximately 4 to 5 mm below the surface of the brainstem at the point when the penetrating array is implanted, and the active stimulating site on electrode 20 is 2.5 mm below the superstructure. It is possible that the patient's brainstem had been significantly distorted by the large vestibular schwannoma. No other electrodes produced any NASE, so a new map

Fig 3: PABI#6 Intensity Discrimination

$\bigcirc$ p13
$\triangle$ p10
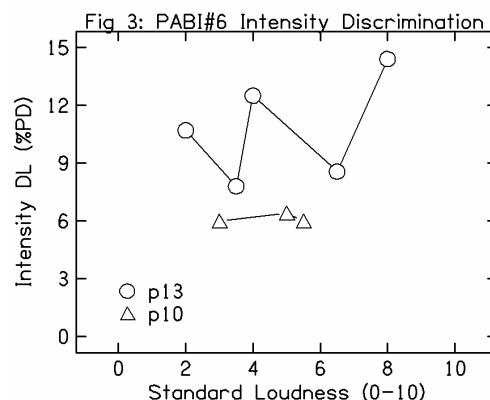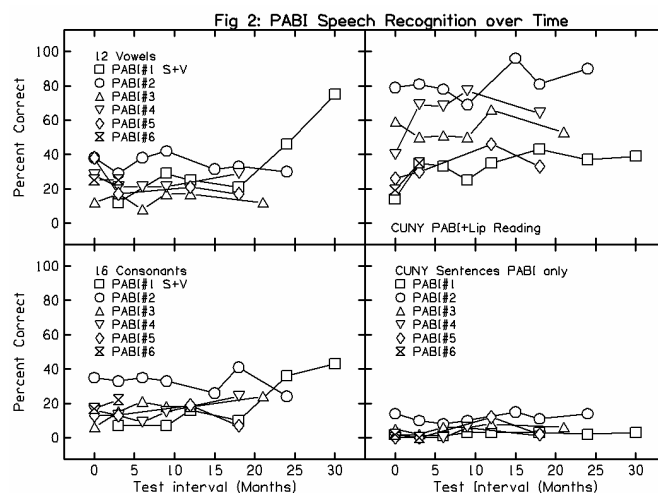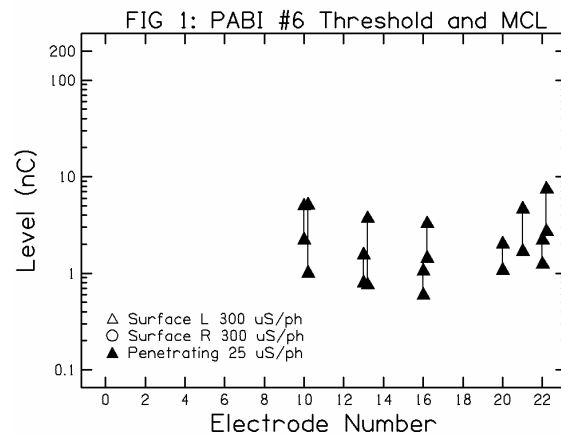
was created without electrode 20. Performance on speech test materials showed no significant change from the levels measured at initial stimulation (Figure 2). However, he has derived benefit from the PABI . His surface electrodes do no produce auditory percepts, so he is the only PABI patient to date who relies entirely on the penetrating electrodes for hearing. Subjectively, the patient reported that walking on gravel sounded just like he remembered with acoustic hearing. Running water sounded okay, but had a strange quality that he could not describe further.

Fig 4: PABI#6 Gap Detection

   Psychophysical testing was conducted on PABI#6 in this quarter: intensity discrimination, gap detection, modulation detection, and forward masking. Figure 3 presents results of intensity discrimination on two penetrating electrodes. Two stimuli were presented and the subject was instructed to select which one was louder. The level of the louder stimulus was adjusted adaptively to track the level at which the louder stimulus was discriminable from the standard at a level of 79% correct. Measures were made on two electrodes as a function of the loudness of the standard stimulus. The results show approximately constant discrimination of about 10% on electrode 13 and 6% on electrode 10. These results suggest that PABI#6 as 10-15 discriminable steps in intensity between threshold and loudness discomfort. These results are not significantly different from intensity discrimination measured in ABI patients with surface electrodes or in patients with cochlear implants.

   Gap detection measures the shortest detectable silent interval in an ongoing sound. Figure 4 presents gap thresholds as a function of the loudness of the ongoing sound from three penetrating electrodes. The hatched area in the figure shows the range of results obtained from cochlear implant listeners and ABI listeners with surface electrodes. Most of the gap detection thresholds from PABI#6 were within this range. PABI#6 required gaps of 20-30 ms for detection at soft levels and less than 10 ms at louder levels.

Fig 5: PABI#6 Modulation Detection

   Modulation detection results from PABI#6 were presented in the last progress report, and additional measures were made in the present quarter. Figure 5 presents new and previous measures of modulation detection as a function of the loudness of the unmodulated carrier stimulus. PABI#6 was able to detect modulation at about -20 dB (10%) on all three penetrating electrodes tested and at all loudness levels. Previous results have shown a significant correlation between modulation detection and speech recognition, with good speech recognition being associated with modulation detection of 3% or smaller. Modulation detection was measured at 10 and 20 Hz - there was no clear difference between the two modulation frequencies.
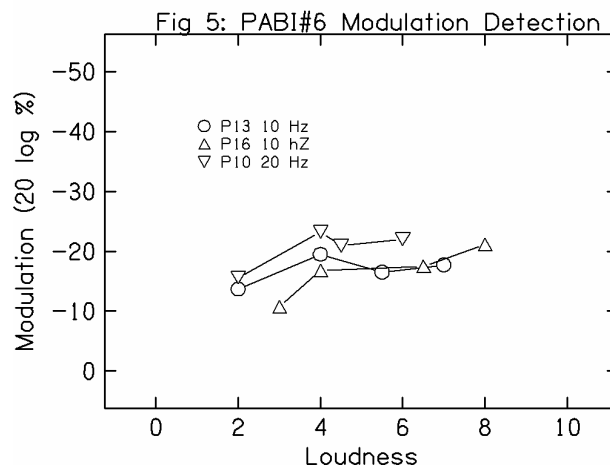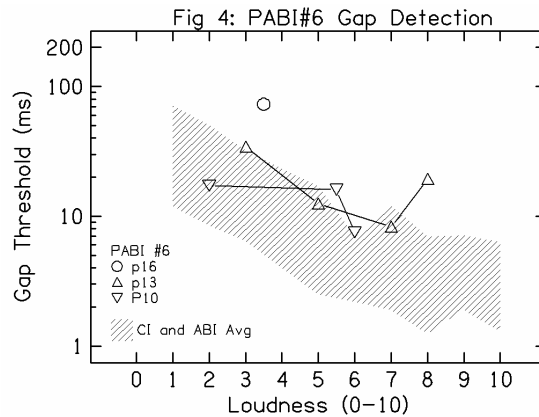
Forward masking measures the recovery from adaptation to a prior stimulus. Figure 6 presents thresholds of a 20 ms probe signal on penetrating electrode 13 as a function of the delay between the probe onset and the offset of a preceding masker. The masker was a 250 pps stimulus, 300 ms in duration and 180 uA, a level that was judged to be a 6 on loudness on a scale of 0-10. The threshold for the brief probe signal was approximately equal to the level of the masker for short probe delays an the threshold recovered as the probe delay increased. No measure of absolute threshold was made for the 20 ms probe during this testing session, but the threshold for a 300 ms burst on electrode 13 was 32 uA and threshold is typically higher for short stimuli. It is likely that the threshold had not recovered completely to the unmasked threshold level by 200 ms following the masker offset.

Overall, the pattern of psychophysical results from PABI#6 was similar to values measured in cochlear implant users and ABI users with surface electrodes.
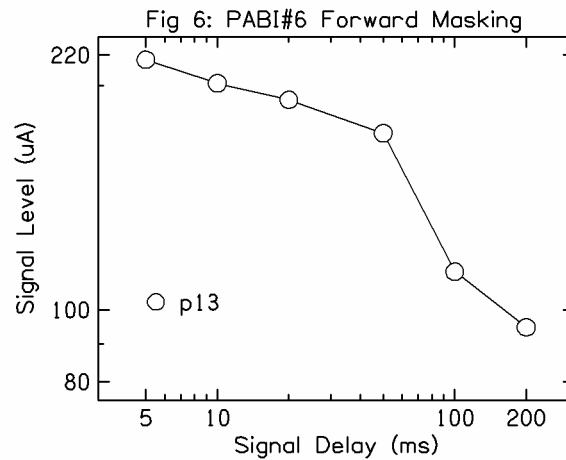
PABI#7

PABI #7 received initial stimulation on 23 May 2006. His threshold and maximum comfortable loudness (MCL) levels are show in Figure 7. Thresholds were high on the lateral end of the electrode array and reached a minimum of 5.5 nC in the middle of the array. He received no auditory sensations on any of the penetrating electrodes, indicating that it had not been inserted into the cochlear nucleus. On penetrating electrodes 20 and 4 he received a similar NASE as PABI#6: sharp pain in the ipsilateral face. Again, the NASE occurred at a stimulation level of 0.25 nC, a level that should not have produced stimulation of neurons remote from the electrode. He also reported strong vertigo from stimulation with surface electrodes and 18. Due to the uncertainty about the cause of the painful stimulation in the face we did not continue testing with PABI#7 and did not give him a speech processor to use. A device integrity test was scheduled for late July to evaluate the function of the implanted receiver/stimulator.
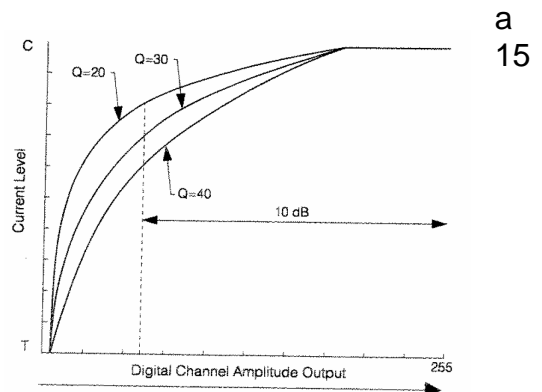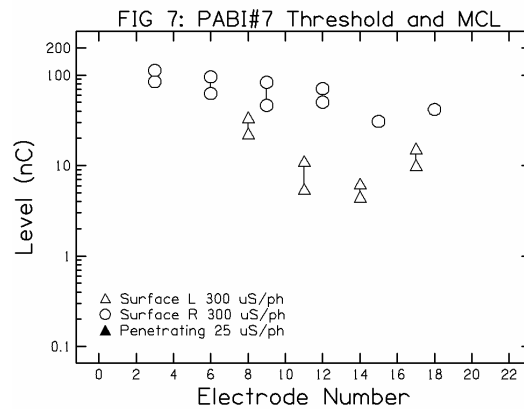
PABI#8

PABI #8 was implanted 30 March 2006 and her initial stimulation was delayed pending the outcome of device integrity testing on PABI #6 and #7.

Improving Modulation Depth

Since modulation detection and speech recognition are linked (Fu, 2004; Colletti and Shannon, 2005), we attempted to improve speech recognition in one patient with a standard ABI and one PABI patient (#3) by changing the loudness mapping function. In the Nucleus CI and ABI system the acoustic envelope magnitudes in each analysis channel are transformed by an approximately logarithmic function before being mapped to electrical output levels. The standard mapping function is designated Q=20 and is slightly more compressive than a logarithmic function (Figure 8). A sinusoidally modulated acoustic sound would be transformed into an electrical waveform that had a more scalloped shape - almost like a sinusoidal wave that had been squared. But theoretically, due to the nature of the loudness growth function for electrical stimulation, the perceptual results should be approximately sinusoidal in terms of loudness. When the value is set to Q=50 the mapping function is more linear. This will have the effect of making low-level sounds softer and high-level sounds louder. A sinusoidally-modulated acoustic signal would now produce stimulus pulses whose amplitude also was approximately sinusoidially modulated. However, again due to the exponential loudness function for electrical stimulation, this will have a perceptual effect that accentuates the peaks of the modulated waveform. The resulting waveform in perceptual terms would look more like a comb - the peaks of the sinusoidal modulation would be greatly exaggerated relative to the middle and low-amplitude portions. Since modulation detection by NF2 patients is significantly poorer than non-tumor patients, this manipulation should enhance the modulation and hopefully improve speech recognition. The results of an acute trial of this altered mapping function on two patients are shown in Figure 9. Speech recognition was tested for single syllable word discrimination, and for vowel and consonant recognition. There was no clear difference in recognition for any of the three tests. Additional patients will be tested with this manipulation and selected patients will receive these "modulation enhancing" processors to use at home for a longer trial period.
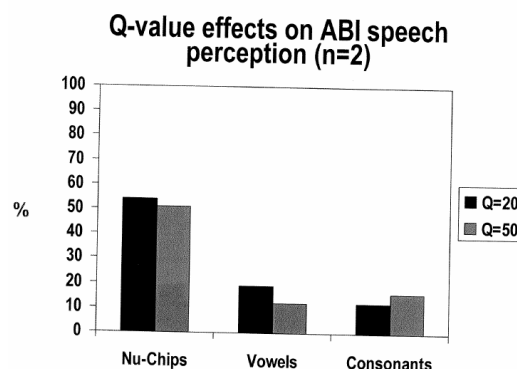
Testing of Non-tumor ABI users

No testing of ABI patients whose deafness was due to causes other the NF2 occurred in this quarter due to an injury that prevented travel. More testing of these patients is scheduled in the next quarter.

Presentations

1annon, RV. (2006). Restoration of hearing by electrical stimulation of the human cochlea, brainstem and midbrain: Implications for speech recognition, *Nobel Mini symposium, Frontiers in Medicine: Cochlear implants – from bench to bedside*, Stockholm, May 11. (invited)

1annon RV, Colletti V, Carner M, Colletti L, Giarbini N (2006). Comparison of ABI Results in NF2 and Non-tumor patients, 9th International Conference on Cochlear Implants. Vienna, June.

References

olletti V and Shannon RV (2005). Open Set Speech Perception with Auditory Brainstem Implant? The Laryngoscope 115:1974-1978.

1, Q.-J. (2002). Temporal processing and speech recognition in cochlear implant users, NeuroReport, 13: 1635-1639.